ACS Medicinal Chemistry Letters

pubs.acs.org/acsmedchemlett

Ranking Ligand Affinity for the DNA Minor Groove by Experiment and Simulation

Kitiyaporn Wittayanarakul,[†] Nahoum G. Anthony,[†] Witcha Treesuwan,[‡] Supa Hannongbua,[‡] Hasan Alniss,[†] Abedawn I. Khalaf,[§] Colin J. Suckling,[§] John A Parkinson,[§] and Simon P. Mackay*,[†]

[†]Strathclyde Institute of Pharmacy and Biomedical Sciences, University of Strathclyde, 27 Taylor Street, Glasgow G4 0NR, United Kingdom, [‡]Chemistry Department and Center of Nanotechnology, Kasetsart University, Bangkok 10900, Thailand, and [§]WestCHEM Department of Pure and Applied Chemistry, University of Strathclyde, 295 Cathedral Street, Glasgow G1 1XL, United Kingdom

ABSTRACT The structural and thermodynamic basis for the strength and selectivity of the interactions of minor groove binders (MGBs) with DNA is not fully understood. In 2003, we reported the first example of a thiazole-containing MGB that bound in a phase-shifted pattern that spanned six base pairs rather than the usual four (for tricyclic distamycin-like compounds). Since then, using DNA footprinting, NMR spectroscopy, isothermal titration calorimetry, and molecular dynamics, we have established that the flanking bases around the central four being read by the ligand have subtle effects on recognition. We have investigated the effect of these flanking sequences on binding and the reasons for the differences and established a computational method to rank ligand affinity against varying DNA sequences.

KEYWORDS Ligand affinity, DNA minor groove, minor groove binders, DNA footprinting, NMR spectroscopy, isothermal titration calorimetry, molecular dynamics

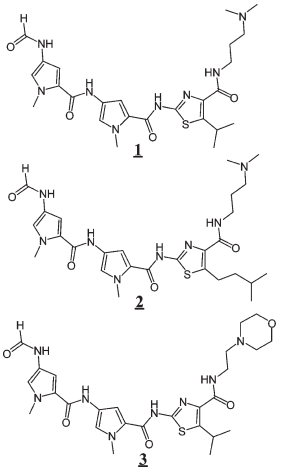

DNA minor groove binders (MGBs) have therapeutic potential in a range of conditions, including cancer and microbial infection. The selectivity of large hairpin polyamide MGBs for specific DNA sequences is well documented,[1] but genuine sequence selectivity for small MGBs is less well established. By better understanding the rules that govern the tight, side-by-side binding of low molecular weight (MW ~ 500) ligands in the DNA minor groove, it should become possible to develop tailored approaches to drug design. The development of MGBs proceeded from the observation that netropsin and distamycin, enabled by their natural isohelicity, bound selectively in the DNA minor groove by a combination of hydrogen bonding with the bases on the groove floor and van der Waals interactions with the groove walls.[2−5] A significant breakthrough in the field came with the observation that a number of MGBs could bind in the minor groove as a side-by-side 2:1 complex[6] with base pair selectivity.[5] While hydrogen bonding to the groove floor endowed specificity for particular sequences, lipophilic interactions with the groove walls were also highly relevant.[7,8] Furthermore, the balance between enthalpic and entropic contributions to MGB binding is the subject of extensive research and appears to vary with both the MGB structure and the binding sequence of the DNA.[9]

Over the past 10 years, we have prepared a library of more than 200 MGBs made up from heterocyclic and head/tail groups that seek to recognize the hydrogen bonding capacity of the groove floor to both achieve specificity and exploit the lipophilic nature of the groove walls to enhance affinity.[10−13] Significantly, we have found that the heterocyclic *N*-alkyl or *C*-alkyl groups can play a crucial role in extending the reading frame of the ligand from four to six base pairs. The first well-characterized example of this effect was our detailed studies by NMR spectroscopy,[11] isothermal calorimetry (ITC), and molecular modeling[14] of the high affinity binding between the DNA duplex d(CGACTAGTCG)$_2$ and thiazotropsin A **1**. Our footprinting data[15] have shown that the generic sequence 5′-**X**CYRG**Z**-3′ forms the reading frame for **1** where **X** is any base except C and **Z** is any base except G. These alterations to the flanking bases of the DNA reading frame for **1** have subtle consequences for binding[15] and have not been explained in structural or energetic terms but have implications for the design of compounds from a medicinal chemistry perspective.

To determine the reasons for this behavior by **1**, we have examined its interaction with oligodeoxynucleotides (ODNs) containing different flanking bases around the central 5′-CTAG-3′ motif using a combination of NMR spectroscopy, ITC, and molecular simulation. We describe for the first time a rapid and

Received Date: March 6, 2010
Accepted Date: July 12, 2010
Published on Web Date: July 30, 2010

DOI: 10.1021/ml100047n | *ACS Med. Chem. Lett.* **2010**, *1*, 376–380

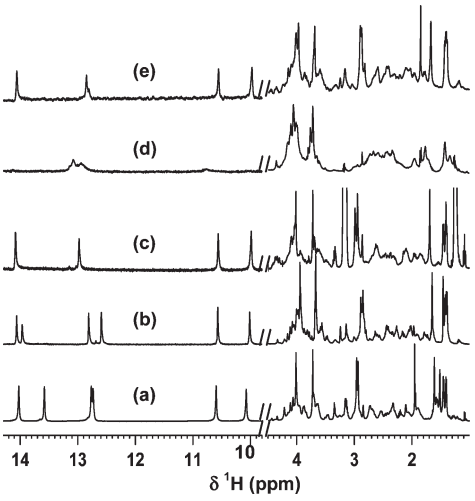

Figure 1. Sections of 1D ^{1}H NMR spectra after mixing 2 mol equiv of thiazotropsin A with the self-complementary oligonucleotides (a) d(CG**A**CTAG**T**CG)$_2$, (b) d(CG**T**CTAG**A**CG)$_2$, (c) d(CG**G**CTAG**C**CG)$_2$, (d) d(CG**C**CTAG**G**CG)$_2$, and (e) d(CG**C**CTAG**I**CG)$_2$.

efficient simulation protocol that can rank the binding affinities for ligands binding 2:1 in a side-by-side fashion.

Analysis of the ^{1}H NMR data for the complex between **1** and 5′-CG**A**CTAG**T**CG-3′ (Figure 1a) had already established that minor groove binding occurs with a staggered 2:1, head-to-tail, side-by-side binding motif[16,17] at the indicated (underlined) reading frame.[11] The same characteristic NMR resonance pattern also occurs for the binding of **1** to both 5′-d(CG**T**CTAG**A**CG)-3′ and 5′-d(CG**G**CTAG**C**CG)-3′ (Figure 1b,c, respectively), all of which produce outstanding quality two-dimensional (2D) nuclear Overhauser effect spectroscopy (NOESY) NMR data sets. In stark contrast, the binding of **1** to 5′-d(CG**C**CTAG**G**CG)-3′ can at best be described as "poor", being characterized by broad NMR resonances (Figure 1d) and ill-defined cross-peaks in 2D NOESY NMR spectra. Our data suggest that while DNA binding occurs between **1** and 5′-**C**CTAG**G**-3′, the complex formed is "loose".

Our evaluation by ITC (for full experimental details, see the Supporting Information) of the binding between **1** and the four different sequences in question confirmed the subtle influences of the CTAG flanking sequences in thermodynamic terms (Figure 2 and Figure S2 and Table S1 in the Supporting Information); the three sequences that produced high quality 2D NOESY NMR data sets had significantly more favorable binding free energies with **1** than 5′-d(CG**C**CTAG**G**CG)-3′, which reflected lower affinity binding by this last sequence observed by NMR. Indeed, the enthalpogram for this sequence when titrated with **1** lacked the characteristic steep inflection curves that characterize minor groove binding ligands with ODNs (Figure 2).[18]

On the basis of the high quality NMR spectra for the efficient binding sequences with **1**, we were able to produce coordinates for the complexes[11] (manuscript in preparation). In the absence of an equivalent data set for **1** binding with 5′-d(CG**C**CTAG**G**CG)-3′, we examined these complexes to identify the reason for poor binding. We recognized the exocyclic amino group of **G**^{8} in the DNA minor groove as creating steric crowding in the vicinity of the dimethylaminopropyl (Dp) tail of **1**. We therefore proposed, like others have done,[19] that removing the **G**^{8} exocyclic NH_2 (i.e., replacement of **G**^{8} in 5′-d(CG**C**CTAG**G**CG)-3′ by inosine, **I**^{8}) would restore the quality of complex formation in a 2:1 mixture with **1**. As the data suggest, the binding between **1** and 5′-d(CG**C**CTAG**I**CG)-3′ falls into the same class as all previous tight binding complexes (Figure 1e). Characteristic patterns in the NMR data (in particular the ^{31}P chemical shift of the phosphorus 3′ to T^{5} at highest ppm, Figure S1 in the Supporting Information) indicate that the complex formed between **1** and 5′-d(CG**C**CTAG**I**CG)-3′ resembles that for 5′-d(CG**A**CTAG**T**CG)-3′. Analysis by ITC confirmed that replacement of **G**^{8} by **I**^{8} in the sequence was thermodynamically favorable for binding **1** (Figure 2 and Table S1 in the Supporting Information) and, in fact, produced the most stable complex of the five sequences. As often encountered with biomolecular interactions, we observed enthalpy−entropy compensation for the binding of **1** to the different ODNs (Figure S3 in the Supporting Information). For systems where the binding appears to be enthalpy driven, this compensation effect might be explained by a strong bonding network that involves the sequestration of water molecules from the disordered bulk (hence unfavorable entropy).[20] For those sequences where entropy became more influential and enthalpy was less prominent, the complex was less conformationally restrained, and the release rather than the ordering of water became more important.

To examine these complexes in more detail, we subjected the solved structures to molecular dynamics (MD) analysis. Our first attempt applied combined MD/MM-PBSA (molecular mechanics Poisson−Boltzmann surface area) calculations to obtain absolute binding free energy data for 2:1 side-by-side binding of a ligand with DNA.[14] To generate experimentally relevant binding simulations for complexation of **1** with the DNA duplex 5′-d(CGACTAGTCG)$_2$-3′, the optimum method relied on a separate trajectory approach (complex and unbound forms simulated separately) using explicit water with the polarizable AMBER force field ff02.[14] The high computational demand of this approach does not readily lend itself to the analysis and comparison of multiple complexes. We therefore explored the use of less expensive implicit MD, which would be applicable to drug discovery programs that contain large libraries of ligands, like our own. We used the coordinates generated by our NMR studies to explore whether implicit MD simulations could reproduce the ranking order of binding for **1** in the tight binding complexes with 5′-d(GCG**A**CTAG**T**CGC)$_2$-3′, 5′-d(GCG**T**CTAG**A**CGC)$_2$-3′, 5′-d(GCG**G**CTAG**C**CGC)$_2$-3′, and 5′-d(GCG**C**CTAG**I**CGC)$_2$-3′. The loose association between 5′-d(GCG**C**CTAG**G**CGC)$_2$-3′ and **1** (Figure 1d) meant that no coordinates were generated for this sequence. To examine the efficiency of different GB (generalized Born) models in AMBER, we compared a standard pair wise descreening GB [HCT, implicit GB (igb) = 1][21] and a modified version by Onufriev and co-workers [OBC(II), igb = 5].[22] A nonpolarizable force-field (FF03)[23] in AMBER was used for all MD simulations. The two GB solvation models (igb = 1 or 5) were applied employing Langevin dynamics with a collision frequency equal to 1 throughout the 10 ns simulations. The temperature was maintained at 300 K. The binding

DOI: 10.1021/ml100047n | ACS Med. Chem. Lett. 2010, 1, 376–380

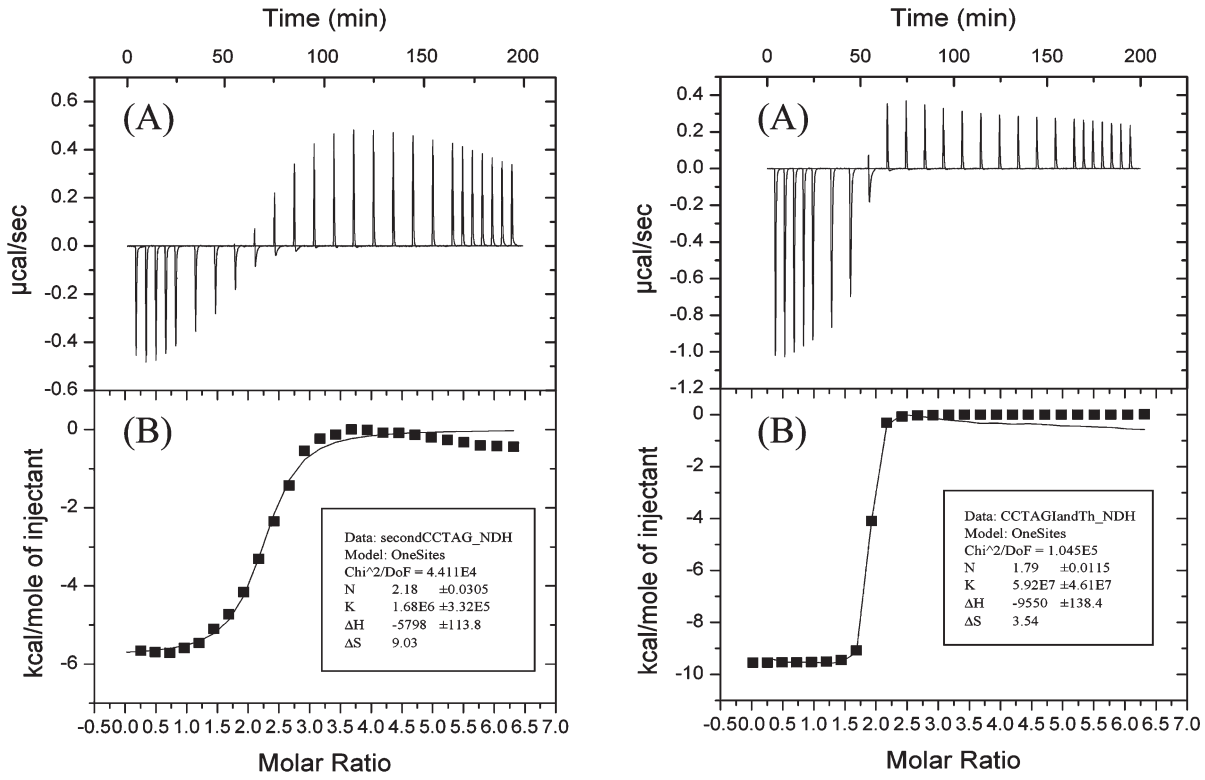

Figure 2. ITC titrations of thiazotropsin A to ODN sequences in PIPES buffer at 25 °C (pH 6.8). (A) Raw data for the titration of thiazotropsin A into d(GCGCCTAGGCGC)$_2$ (left) and d(GCGCCTAGICGC)$_2$ (right). (B) Enthalpogram retrieved from A and corrected for the heat of dilution; the line represents the least-squares fit to a single-site binding model.

free energies were the average of 100 snapshots taken from the last 5 ns of the implicit MD simulations. Only 10 snapshots from the last nanosecond period were kept for normal mode analysis (NMA) to evaluate the entropy. The full simulation protocols can be found in the Supporting Information.

Our NMR and ITC studies indicated the presence of only the 2:1 complex structure during titration with the ligand; indeed, all of our experimental studies have thus far found no evidence for the formation of an initial 1:1 complex prior to 2:1 binding and that thiazotropsin type ligands behave like head-to-tail dimers in solution, and monomers are not present at the ligand concentrations under investigation.[24] In line with our previous study, we have therefore used the thermodynamic cycle represented in Figure 3 and expressed the parameters that can be calculated using the MM-PBSA methodology to obtain binding free energies of ligands with various ODNs by solving eqs 1−3.

$$\Delta G_{b} = \Delta G_{association} + \Delta\Delta G_{sol} \quad (1)$$

$$\Delta G_{association} = \Delta H_{association} - T\Delta S_{association}$$
$$\Delta H_{association} = \Delta E_{MM}{}^{DL_2} \quad (2)$$
$$-T\Delta S_{association} = -T\Delta S^{DL_2}$$

$$\Delta\Delta G_{sol} = \Delta G_{sol}{}^{DL_2} - \Delta G_{sol}{}^{D} - \Delta G_{sol}{}^{L_2} \quad (3)$$

Comparison of the experimental and simulated relative free energies (ΔG_{rel})[25] of the ligand dimer binding with DNA is shown in Figure 4 (actual experimental and theoretical values are summarized in Table 1 and Table S2 in the Supporting Information). Our results indicate that ΔG_{rel} from the implicit MD simulations (igb = 5) of the single trajectory reproduced the ranking order of affinity (CCTAGI > ACTAGT > TCTAGA > GCTAGC) and represents the first report of a simulation method that can rank 2:1 ligand binding free energies in line with experiment. Furthermore, it is also computationally efficient, running 14 times faster than explicit MD (using 16 processors in parallel on the UK National Grid Service computers). The method using igb = 1 ranked the CCTAGI containing system as having the worst affinity but kept the other three sequences in the correct order (ACTAGT > TCTAGA > GCTAGC > CCTAGI). On the basis of these results, only the more recent implementation (igb = 5) was developed further.

Finally, to determine whether our simulation protocol could rank affinities for related ligands, we calculated the binding energies for two analogues of thiazotropsin A (**2** and **3**), which we investigated by ITC, but not by NMR. The preparation of **1** and **3** has been described previously,[10,13] while details for the preparation and characterization of **2** can be found in the Supporting Information. The implicit MD simulations (igb = 5) yielded ΔG_{rel} values of −5.0 and −9.8 kcal/mol for analogues **2** and **3**, respectively, bound to the ACTAGT containing ODN, and their ranking reflects the values obtained by ITC (Figure 4 and Table 2).

Examination of the absolute enthalpic (ΔH_{abs}), entropic ($T\Delta S_{abs}$), and free energy (ΔG_{abs}) terms of 5′-d(GCGACTAGTGCG)$_2$-3′ binding to **1**−**3** obtained from both simulation

DOI: 10.1021/ml100047n | ACS Med. Chem. Lett. 2010, 1, 376–380

ACS Medicinal Chemistry Letters
pubs.acs.org/acsmedchemlett

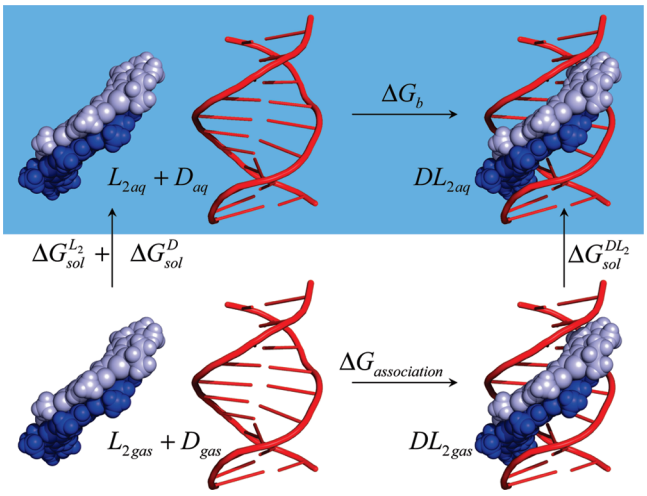

Figure 3. Thermodynamic cycle for the association of the thiazotropsin A dimer (L_2, shades of blue) with duplex 5′-d(GCGACTAGTCGC)$_2$-3′ (D, red).

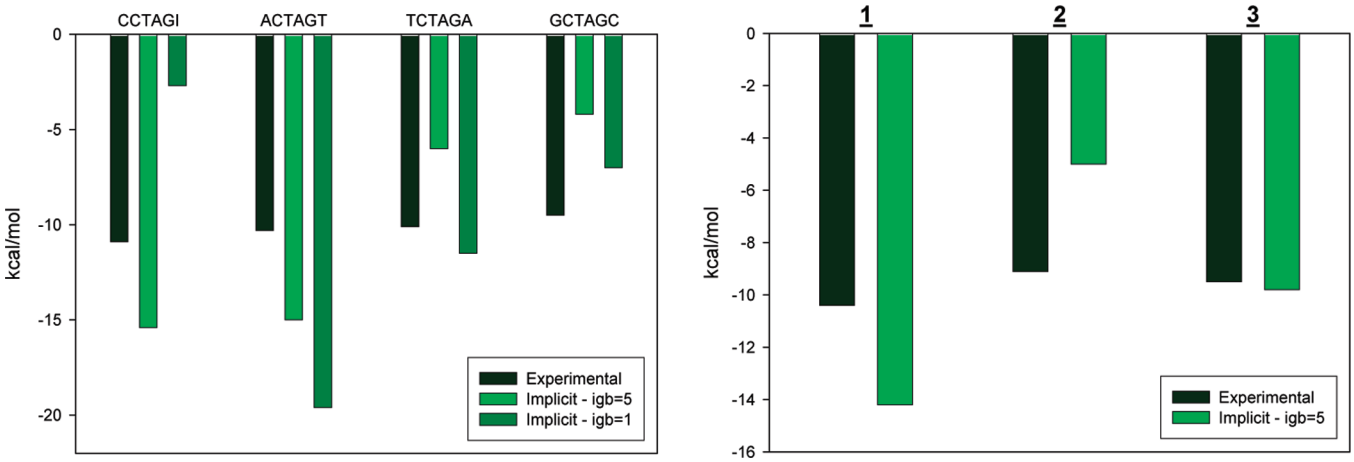

Figure 4. Left: relative binding free energies for **1** bound to the different ODNs based on experiment and implicit MD using igb = 1 and igb = 5. Right: relative binding free energies of **1**, **2**, and **3** binding to d(GCGACTAGTCGC)$_2$.

Table 1. Individual Enthalpic, Entropic, and Free Energy Terms Obtained from the Experiments and Calculations for **1** Binding with Four Different ODNs[a]

	ODN sequence			
energy term	CCTAGI	ACTAGT	TCTAGA	GCTACG
ΔH	−79.3	−78.5	−83.7	−84.9
$T\Delta S$	−23.3	−22.9	−37.0	−40.0
ΔG_{abs}	−56.1	−55.6	−46.7	−44.9
ΔG_{rel}	−15.4	−15.0	−6.1	−4.2
ΔG_{exp}	−10.9	−10.3	−10.1	−9.5

[a] $\Delta G_{rel} = \Delta G_{abs} - \text{shift}$. $\text{Shift} = [\sum_{i=1}^{\text{DNAsequence}} (\Delta G_{abs} - \Delta G_{exp})_i]/n = -40.6$.

Table 2. Energy Contributions of **1**, **2**, and **3** Binding to d(GCGACTAGTCGC)$_2$ Using Implicit MD (igb = 5) and the Experimental Data (ITC Method)[a]

	experimental			simulated		
energy term	**1**	**2**	**3**	**1**	**2**	**3**
ΔH	−12.8	−14.3	−15.6	−78.5	−82	−90.3
$T\Delta S$	−2.4	−5.2	−6.1	−22.9	−35.5	−39.0
ΔG_{abs}	−10.4	−9.1	−9.5	−55.6	−46.5	−51.3
ΔG_{rel}				−14.2	−5.0	−9.8

[a] All of the values are in kcal/mol.

and experiment can help provide insight into the drug design process. According to Table 2, despite the isopentyl group being enthalpically favorable through enhanced lipophilic contacts in accordance with our design paradigm, the greater flexibility of this chain generates a greater entropic penalty on binding than is compensated by enhanced lipophilic interactions and thus reduces the binding affinity of **2** for the ODN. Similarly, comparison of **1** with **3** shows that replacing the dimethylamino propyl tail with a morpholino ethyl group is more favorable enthalpically through hydrogen bonding between the morpholine oxygen and the ODN, but again, the entropic penalty negates this enthalpic gain.

In conclusion, while our aim is to enhance DNA recognition through enhanced lipophilic interactions, the subtlety of DNA recognition continues to be strongly influenced by

DOI: 10.1021/ml100047n | ACS Med. Chem. Lett. 2010, 1, 376–380

favorable matching of three-dimensional shape, hydrogen bond partnering, and conformational considerations. We believe that the information provided by this detailed study will be important in informing the design and implementation of modeling parameters capable of identifying potentially "good" and "bad" binders on the basis of the structural features observed here.

SUPPORTING INFORMATION AVAILABLE

Computational and experimental details. This material is available free of charge via the Internet at http://pubs.acs.org.

AUTHOR INFORMATION

Corresponding Author: *To whom correspondence should be addressed. Tel: +44(0)1415482866. Fax: +44(0)1415522562. E-mail: simon.mackay@strath.ac.uk.

Funding Sources: We thank the Royal Golden Jubilee Ph.D. Program (3C.KU/47/B.1) and the Thailand Research Fund for support of W.T. and EPSRC and the Scottish Funding Council for their funding of the Physical Organic Chemistry initiative at Strathclyde.

ACKNOWLEDGMENT

We thank the National Grid Service for access to cluster facilities.

REFERENCES

(1) Dervan, P. B.; Edelson, B. S. Recognition of the DNA minor groove by pyrrole-imidazole polyamides. *Curr. Opin. Struct. Biol.* **2003,** *13*, 284–289.
(2) Kopka, M. L.; Yoon, C.; Goodsell, D.; Pjura, P.; Dickerson, R. E. The molecular origin of DNA-drug specificity in netropsin and distamycin. *Proc. Natl. Acad. Sci. U.S.A.* **1985,** *82*, 1376–1380.
(3) Mrksich, M.; Wade, W. S.; Dwyer, T. J.; Geierstanger, B. H.; Wemmer, D. E.; Dervan, P. B. Antiparallel side-by-side dimeric motif for sequence-specific recognition in the minor groove of DNA by the designed peptide 1-methylimidazole-2-carboxamide netrosin. *Proc. Natl. Acad. Sci. U.S.A.* **1992,** *89*, 7586–7590.
(4) Patel, D. J. Antibiotic-DNA interactions: Intermolecular nuclear Overhauser effects in the netropsin-d(CGCGAATTCGCG) complex in solution. *Proc. Natl. Acad. Sci. U.S.A.* **1982,** *79*, 6424–6428.
(5) Wade, W. S.; Mrksich, M.; Dervan, P. B. Design of peptides that bind in the minor groove of DNA at 5′-(A,T)G(A,T)C(A,T)-3′ sequences by a dimeric side-by-side motif. *J. Am. Chem. Soc.* **1992,** *114*, 8783–8794.
(6) Pelton, J. G.; Wemmer, D. E. Structural characterization of a 2:1 distamycin A/d(CGCAAATTGGC) complex by two-dimensional NMR. *Proc. Natl. Acad. Sci. U.S.A.* **1989,** *86*, 5723–5727.
(7) Lane, A. N.; Jenkins, T. C. Thermodynamics of nucleic acids and their interactions with ligands. *Q. Rev. Biophys.* **2000,** *33*, 255–306.
(8) Misra, V. K.; Honig, B. On the magnitude of the electrostatic contribution to ligand-DNA interactions. *Proc. Natl. Acad. Sci. U.S.A.* **1995,** *92*, 4691–4695.
(9) Chaires, J. B. A thermodynamic signature for drug-DNA binding mode. *Arch. Biochem. Biophys.* **2006,** *453* (1), 26–31.
(10) Anthony, N. G.; Fox, K. R.; Johnston, B. F.; Khalaf, A. I.; Mackay, S. P.; McGroarty, I. S.; Parkinson, J. A.; Skellern, G. G.; Suckling, C. J.; Waigh, R. D. DNA binding of a short lexitropsin. *Bioorg. Med. Chem. Lett.* **2004,** *14* (5), 1353–1356.
(11) Anthony, N. G.; Johnston, B. F.; Khalaf, A. I.; MacKay, S. P.; Parkinson, J. A.; Suckling, C. J.; Waigh, R. D. Short lexitropsin that recognizes the DNA minor groove at 5′-ACTAGT-3′: Understanding the role of isopropyl-thiazole. *J. Am. Chem. Soc.* **2004,** *126* (36), 11338–11349.
(12) Khalaf, A. I.; Ebrahimabadi, A. H.; Drummond, A. J.; Anthony, N. G.; Mackay, S. P.; Suckling, C. J.; Waigh, R. D. Synthesis and antimicrobial activity of some netropsin analogues. *Org. Biomol. Chem.* **2004,** *2* (21), 3119–3127.
(13) Anthony, N. G.; Breen, D.; Clarke, J.; Donoghue, G.; Drummond, A. J.; Ellis, E. M.; Gemmell, C. G.; Helesbeux, J. J.; Hunter, I. S.; Khalaf, A. I.; Mackay, S. P.; Parkinson, J. A.; Suckling, C. J.; Waigh, R. D. Antimicrobial lexitropsins containing amide, amidine, and alkene linking groups. *J. Med. Chem.* **2007,** *50* (24), 6116–6125.
(14) Treesuwan, W.; Wittayanarakul, K.; Anthony, N. G.; Huchet, G.; Alniss, H.; Hannongbua, S.; Khalaf, A. I.; Suckling, C. J.; Parkinson, J. A.; Mackay, S. P. A detailed binding free energy study of 2: 1 ligand-DNA complex formation by experiment and simulation. *Phys. Chem. Chem. Phys.* **2009,** *11* (45), 10682–10693.
(15) James, P. L.; Merkina, E. E.; Khalaf, A. I.; Suckling, C. J.; Waigh, R. D.; Brown, T.; Fox, K. R. DNA sequence recognition by an isopropyl substituted thiazole polyamide. *Nucleic Acids Res.* **2004,** *32* (11), 3410–3417.
(16) Trauger, J. W.; Baird, E. E.; Mrksich, M.; Dervan, P. B. Extension of sequence-specific recognition in the minor groove of DNA by pyrrole-imidazole polyamides to 9−13 base pairs. *J. Am. Chem. Soc.* **1996,** *118*, 6160–6166.
(17) Kopka, M. L.; Goodsell, D.; Han, G. W.; Chiu, T. K.; Lown, J. W.; Dickerson, R. E. Defining GC-specificity in the minor groove: Side-by-side binding of the di-imidazole lexitropsin to C-A-T-G-G-C-C-A-T-G. *Structure* **1997,** *5*, 1033–1046.
(18) Freyer, M. W.; Buscaglia, R.; Nguyen, B.; Wilson, W. D.; Lewis, E. A. Binding of netropsin and 4,6-diamidino-2-phenylindole to an A(2)T(2) DNA hairpin: A comparison of biophysical techniques. *Anal. Biochem.* **2006,** *355* (2), 259–266.
(19) Bailly, C.; Waring, M. J. Transferring the purine 2-amino group from guanines to adenines in DNA changes the sequence-specific binding of antibiotics. *Nucleic Acids Res.* **1995,** *23* (6), 885–892.
(20) Syme, N. R.; Dennis, C.; Bronowska, A.; Paesen, G. C.; Homans, S. W. Comparison of entropic contributions to binding in a "hydrophilic" versus "hydrophobic" ligand-protein interaction. *J. Am. Chem. Soc.* **2010,** *132*, 8682–8689.
(21) Hawkins, G. D.; Cramer, C. J.; Truhlar, D. G. Parametrized models of aqueous free energies of solvation based on pairwise descreening of solute atomic charges from a dielectric medium. *J. Phys. Chem.* **1996,** *100* (51), 19824–19839.
(22) Feig, M.; Onufriev, A.; Lee, M. S.; Im, W.; Case, D. A.; Brooks, C. L. Performance comparison of generalized born and Poisson methods in the calculation of electrostatic solvation energies for protein structures. *J. Comput. Chem.* **2004,** *25* (2), 265–284.
(23) Duan, Y.; Wu, C.; Chowdhury, S.; Lee, M. C.; Xiong, G. M.; Zhang, W.; Yang, R.; Cieplak, P.; Luo, R.; Lee, T.; Caldwell, J.; Wang, J. M.; Kollman, P. A point-charge force field for molecular mechanics simulations of proteins based on condensed-phase quantum mechanical calculations. *J. Comput. Chem.* **2003,** *24* (16), 1999–2012.
(24) Hamdan, I.; Skellern, G. G.; Waigh, R. D. Use of capillary electrophoresis in the study of ligand-DNA interactions. *Nucleic Acids Res.* **1998,** *26*, 3053–3058.
(25) Wittayanarakul, K.; Hannongbua, S.; Feig, M. Accurate prediction of protonation state as a prerequisite for reliable MM-PB(GB)SA binding free energy calculations of HIV-1 protease inhibitors. *J. Comput. Chem.* **2008,** *29* (5), 673–685.

DOI: 10.1021/ml100047n | *ACS Med. Chem. Lett.* **2010,** *1*, 376–380